Basin Research (1999) **11,** 7–19

The generation and degradation of marine terraces

R. S. Anderson,* A. L. Densmore† and M. A. Ellis‡

**Department of Earth Sciences and Institute for Tectonics, University of California, Santa Cruz, CA 95064, USA*
†Department of Geology, Trinity College, Dublin 2, Ireland
‡Center for Earthquake Research and Information, The University of Memphis, TN 38152, USA

ABSTRACT

Marine terraces are ephemeral planar landforms. While tectonic and climatic forcings responsible for the generation of existing marine terraces have operated for at least 1 Myr, terraces have been completely removed by erosion above a given altitude (and hence above a given age). Above this altitude, the landscape has forgotten that it was once terraced. We ask what controls this characteristic time-scale, which we term the 'forget time', in a landscape. We approach the problem with simple scaling arguments, and 1-D numerical models of landscape evolution.

Using a simple cliff erosion model with a realistic sea-level history, rock uplift and a cliff retreat rule, we find that the most important means of terrace removal is through the deeper transgression of a subsequent sea cliff into the landmass. The sequence of preserved terraces depends upon the history of sea cliff incursion into the landmass. The extent of sea cliff incursion depends on the duration of the sea-level highstand, the far-field wave energy input and the degree to which bathymetric drag dissipates wave energy. This portion of the marine terrace survival problem is an example of a common problem in geomorphology, in which the record of past tectonic or climatic events is rendered incomplete by the potential for younger events to wipe the topographic slate clean.

While sea cliffs decay through time, their form can still be recognized many hundreds of thousands of years after formation. This reflects the diffusive nature of their decay: early rapid evolution and lowering of maximum slopes yields to slower rates through time. Incision by streams, on the other hand, is rapid, as the streams respond to base-level history driven by sea-level changes. The rate of incision reflects the local climate conditions, and is limited by the rate of base-level fall.

The principal means of vanquishing a marine terrace is by backwearing of slopes adjacent to these incising streams. The forget time should be proportional to the spacing between major incising streams and to the angle of hillslope stability, and should be inversely proportional to the rate of channel incision. This yields an overestimate of the forget time, as the terraced interfluves are reduced as well by the headward incision of tributary streams.

The resulting landscape may be viewed as a terraced fringe separating the sea from the fully channellized landscape. Over time-scales corresponding to many glacial–interglacial sea-level oscillations, this fringe can achieve a nearly steady width. The rate of generation of new terraced landscape, reflecting the uplift rate pattern, is then balanced by the rate at which the terraces are erased beyond recognition by channel and hillslope processes. The width of this fringe should depend upon the precipitation, and upon the distance to the nearest drainage divide, both of which limit the maximum power available to drive channel incision.

INTRODUCTION

Mountains result from arguments between tectonic and geomorphic processes. The tectonic forcing generates a rock uplift pattern that reflects, for example, slip on crustal faults, or the strain-rate field in ductile materials at greater depth. The geomorphic processes that dictate the incision of the finer scale topography into the rising landmass are modulated by both the slopes and the altitudes produced by the tectonic uplift pattern, by

Fig. 1. Air photograph of the marine terraced coastline north of Santa Cruz, California, showing three well-developed planar platforms near the coast, giving way to more steep-sided channel networks in the mountains behind that typify the remainder of the landscape. The toe of the small stream that exits to the coast in the left of the photograph is alluviated, although locally bridged by Highway 1. Note as well the many abandoned channels that fail to incise to sea-level, but that instead exit onto the next lower terrace platform.

climatic controls that dictate the delivery of moisture and by fluctuations in the ultimate base-level of the system, generally in the form of sea- or lake level. Rarely does the geomorphologist have markers in the landscape that allow detailed assessment of the rates of both geomorphic and tectonic processes. More commonly, we seek landscapes that have achieved a steady-state form, in which the tectonic and geomorphic processes have become balanced, where the measurement of one rate will allow the calculation of the other.

Wave-cut marine terraces represent a stark contrast to this situation, as they result in a coastal landscape which looks very different near the coast than it does a few kilometres inland (Fig. 1). The kilometre-wide flat interfluves of the terrace platforms give way to more typical sharp-crested interfluves within 5 km of the coast. While we might be tempted to assume that this nonuniformity in the landscape reflects a temporal nonsteadiness in the processes that have shaped it, we argue that there are characteristic time and length scales for both the production and the removal of the terraced flats. The few-kilometre-wide terraced fringe of a coastal landscape thus maintains a consistent gross morphology through time, despite the fact that the terraces themselves are continually evolving in both space and time. Viewed at a coarse enough scale, in which we ignore the details of the timing of the platform sequence, these may indeed be steady-state landscapes, maintaining a relatively constant-width fringe of terraced land separating the sea from the nonbenched massif landward. In this paper, we ask what determines the size of this terraced fringe.

A wave-cut platform is etched into a landscape whenever erosion by waves drives a sea cliff landward (e.g. Bradley & Griggs, 1976). This platform is then abandoned by the sea when sea-level declines (predominantly during ice sheet growth in the Quaternary), leaving behind a terrace deposit of beach sand or gravel that thinly mantles the bench (Bradley, 1957). If by the time the sea-level reaches a subsequent highstand the landmass has risen sufficiently, the old wave-cut platform will be left high and dry, and a new platform will be etched into the landmass at a lower altitude. The diachroneity of a terrace surface records the duration of sea-level highstand, and the age of the inner edge reflects the abandonment of the highstand beach at the beginning of the subsequent fall in sea-level. A flight of marine terraces therefore records a history of a rising landmass in the face of fluctuating sea-level. Numerous studies have used marine-terraced landscapes for their record of tectonic uplift, for their record of sea-level fluctuation or for their record of landscape evolution subsequent to abandonment by the sea. In particular, a few studies have employed simple one- and two-dimensional numerical models for terrace development (e.g. Turcotte & Bernthal, 1984, in the construction of coral terraces; Rosenbloom & Anderson, 1994; Cinque *et al*., 1995, for erosional coastlines). One of the themes of this paper is that 'memory' of past events in this terraced landscape is imperfect for several reasons, and that such landscapes are but one of several examples of 'memory loss' in the geomorphic record.

Our approach is broken into several parts (Fig. 2). Before engaging in a discussion of the degradation of marine terraced landscapes, we must first discuss terrace origin. Here we will stress the possibility that a young terrace can obliterate portions of the record by eroding sufficiently into the landscape to destroy an older terrace. Once a terrace has been created, it is also attacked subaerially, resulting in degradation of the palaeo-sea cliffs, and incision of river channels into the landscape. Both processes reduce the distinctive features of the platforms – the first by softening the once-sharp edges of the cliffs, the second by allowing side-valley walls to eat laterally into the platform edges. While this work is motivated primarily by observations of the relatively well-studied flight of terraces near Santa Cruz, California, from which we derive representative tectonic and geomorphic process rates, the conclusions drawn can be applied to other coastlines.

GENERATION OF MARINE TERRACE PLATFORMS

Sea cliff retreat generates wave-cut platforms. The locus of wave attack is the line at which the plane defined by

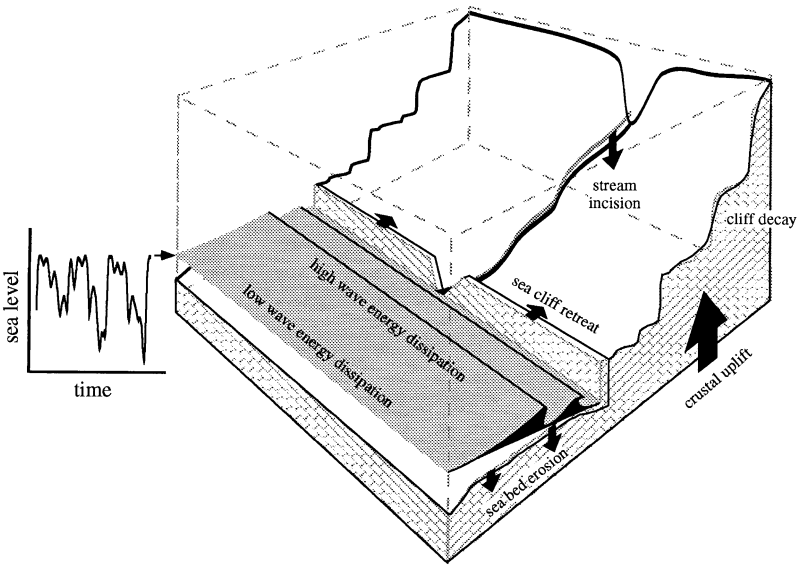

Fig. 2. Schematic diagram of the elements of the evolution of the marine terraced fringe of a rising landmass. The landmass is rising relative to some fixed datum owing to tectonic processes. Sea-level is fluctuating (curve at left) with an amplitude of 120 m over glacial cycles in the late Quaternary. The instantaneous intersection of the sea with the land dictates the locus of wave attack, forcing cliff retreat, the rate of which is determined by the wave energy reaching the coast, and the erodibility of the landmass. Energy is extracted from the approaching waves by interaction with the sea bed, at low rates where the water is deep (relative to the wave height), and at high rates in shallow water (see Fig. 4). Once emerged, the landmass is attacked by surface processes that drive both degradation of the sea cliffs, and incision of the streams into the bedrock.

the sea surface intersects the complex topography of the landmass. Relative motion between the landmass and the sea surface is driven by diverse processes – motion of the land by tectonics, and eustatic sea-level by global-scale climate change, principally through the sequestering of ocean water in ice sheets, and the subsequent release of water upon their melting. The rate of sea cliff retreat, in turn, is a complicated function of wave energy and delivery to the shoreline, topography, bathymetry, lithology and the specific processes of erosion. Below, we consider the controls on both of these concepts – the locus and rate of sea cliff retreat.

Controls on the land–sea intersection

Uplift of rock can be smooth or jerky, can vary significantly in space and can result from a number of physical processes. Most commonly, uplift results from convergent tectonics and subsequent isostatic adjustments to erosion, although bends and displacement gradients associated with strike slip faults can also drive rock uplift. We restrict our attention to sites in which the uplift is relatively uniform along the coast, and is smooth, meaning that the uplift in any single seismic event is small relative to the total vertical displacement between subsequent sea-level highstands.

Sea-level history is known only imperfectly, and is best constrained at its local maxima and minima. The approximate timing of the sea-level fluctuations is known through the oxygen isotopic record from deep sea forams, which is thought to record largely ice volume history (e.g. Shackleton & Opdyke, 1973). More elusive are the magnitude and the rates of the sea-level swings. The most well-documented portion of the sea-level record is that associated with the close of the last glacial maximum (LGM), in which both ages and palaeo-sea-level are obtained from submerged shallow-water corals in Barbados (Fairbanks, 1989; Bard *et al.*, 1990). Unfortunately, to reconstruct Quaternary terrace sequences, we must have a sea-level record that encompasses several highstands, and thus several glacial–interglacial cycles. We use ages and heights of sea-level highstands from the rising coastline of the Huon Peninsula of Papua New Guinea (Chappell & Shackleton, 1986). A scatter plot of many $\delta^{18}O$ – sea-level pairs (Fig. 3a) suggests the following transformation between the $\delta^{18}O$ record and sea-level (SL), the former available through the Imbrie *et al.* (1984) compilation:

$$SL = -32.841 - (33.747\ \delta^{18}O) - (8.5605\ (\delta^{18}O)^2). \quad (1)$$

This relationship results in the time series of sea-level shown in Fig. 3(b). We note that this transformation does a better job at producing a sea-level history than does a linear transformation of the $\delta^{18}O$ record (thin line, Fig. 3b). We are well aware that the benthic $\delta^{18}O$ record reflects not only ice volume (and hence sea-level) but bottom water temperature fluctuations as well (e.g. Shackleton & Opdyke, 1973). In addition, even if it were a perfect recorder of ice volume, the transformation to sea-level must include information about the hypsometry of the oceans. While one may argue that this effect is minimal (the area of the continental shelves exposed during lowstands is trivial compared with the area of the oceans), thermal expansion of warmed seawater on the shelves may introduce significant error. Finally, we note that there are no reliable independent ages constraining the $\delta^{18}O$ curve beyond 200 ka. However, we emphasize that as our goal here is not to reproduce the details of a particular terrace sequence, but to illustrate the variety of processes involved in generating a terraced coastline,

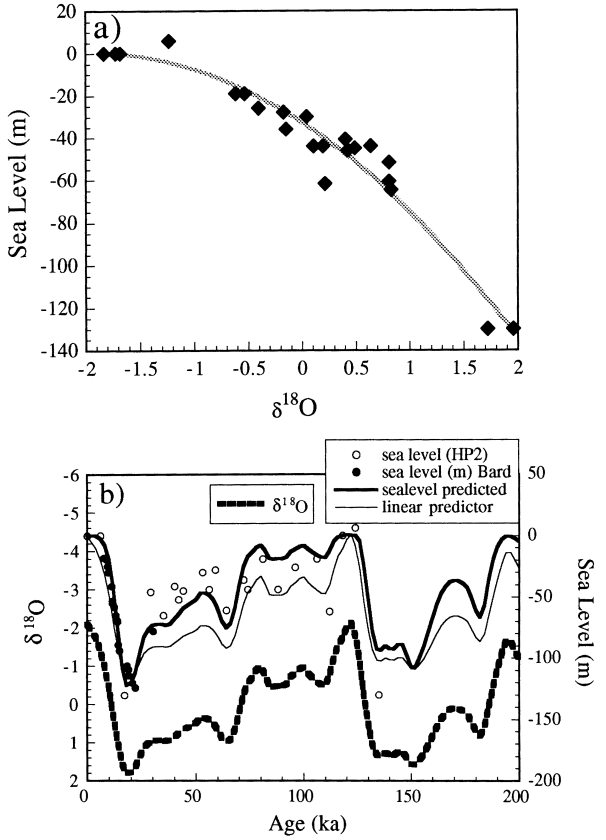

Fig. 3. Determination of the sea-level history from a continuous oxygen isotope record. (a) Scatterplot of the estimated sea-levels from work on the Huon Peninsula of Papua New Guinea and the associated deep-sea benthic foram-based $\delta^{18}O$ record, here from the stacked, normalized record reported by Imbrie *et al.* (1984). (b) Sea-level and $\delta^{18}O$ as functions of time before present. The $\delta^{18}O$ record (bold, dashed line) is the stacked, normalized record (Imbrie *et al.*, 1984). The closed circles are data from the detailed documentation of sea-level from corals in Barbados (Fairbanks, 1989; Bard *et al.*, 1990), while the open circles are from dated corals on Huon Peninsula emergent terraces (Chappell & Shackleton, 1986). A linear prediction from the $\delta^{18}O$ curve (thin solid line) underpredicts the amplitude of the sea-level swings in times of intermediate $\delta^{18}O$ values. We prefer the nonlinear predictor (thick solid line) based upon the best fit to the data shown in (a).

all of these errors in the sea-level history are not fatal to the exercise. This sea-level history, combined with the uplift rate of the landmass, yields a time series of the locus of wave attack on the coastline.

Controls on sea cliff erosion

Cliff erosion, and hence extension of the wave-cut platform, occurs through a variety of processes. We focus here on those driven directly by the wave attack. Ultimately, the cliffs are attacked by impacting waves in which sediment is embedded. As in incision of rivers into bedrock, the processes are varied, ranging from abrasion by grains embedded in the flow (waves), to quarrying of blocks, to enhanced weathering of the rock subaerially (e.g. Hancock *et al.*, 1998). Along the Santa Cruz coastline, bedrock is typically Tertiary sandstone and mudstone, and chemical dissolution of the rock or the cement is not important. Erosion is accomplished either by block removal or by grain-by-grain abrasion. Both of these processes are strong functions of the wave energy arriving at the cliff base, and therefore depend upon the far-field wave climate, the bathymetry that dictates how much of that wave energy makes it to the cliff, and the resistance or susceptibility of the cliff to erosion, relating wave energy to erosion rate (e.g. Bradley, 1957; Bradley & Griggs, 1976).

We scale an erosion rate through use of measured rates along the coastline north of Santa Cruz, which vary greatly but are of the order of several tens of centimetres per year (Best & Griggs, 1991). The spatial pattern of erosion is dictated by the tidal range, which smears the locus of wave attack vertically, and the expected spatial distribution of wave energy along the sea bed. Wave energy decays with depth at a length scale dictated by the wavelength; beyond a depth equal to several times the wavelength, water particle motions are too small to accomplish significant work on the sea floor. A plausible expression for the water-depth dependence of the sea bed erosion rate is a linear function of the rate of energy dissipation against the sea bed (e.g. Sunamura, 1992):

$$\mathrm{d}z/\mathrm{d}t = \beta\ (\mathrm{d}E/\mathrm{d}t) = \beta\ (\mathrm{d}E/\mathrm{d}t)_0 \exp(-h/h^*) \qquad (2)$$

where $\mathrm{d}z/\mathrm{d}t$ is the vertical sea bed erosion rate, $\mathrm{d}E/\mathrm{d}t$ is the energy dissipation rate, $(\mathrm{d}E/\mathrm{d}t)_0$ is the rate of wave energy dissipation in very shallow water, h is water depth to the local sea floor, h^* is the water depth at which the dissipation rate is 1/e of that in very shallow water. Noting that wave base, h_{wb}, is that depth at which dissipation rate is essentially zero, we can set $h^* = h_{wb}/4$. Connecting this to the wave climate, the dissipation depth scale h^* is of the order of the wavelength. The constant, β, is an efficiency factor relating energy dissipation rate to erosion rate.

Wave energy is dissipated all along the trajectory of an approaching wave. In order to calculate that energy remaining to drive cliff erosion, we must integrate the dissipation rate over the shelf. There is no dissipation of energy until the water depth is less than h_{wb}. At shallower depths, the wave energy declines with distance at a rate that increases exponentially as the local depth, h, declines (Fig. 4). Using the chain rule to relate temporal changes in dissipation rate to spatial changes,

$$\mathrm{d}E/\mathrm{d}t = (\mathrm{d}E/\mathrm{d}x)\ (\mathrm{d}x/\mathrm{d}t) = V\ \mathrm{d}E/\mathrm{d}x, \qquad (3)$$

where V is the component of wavespeed normal to the coast, then we may use eqn 2 to write

$$\mathrm{d}E/dx = (1/V)\ (\mathrm{d}E/\mathrm{d}t)_0 \exp(-4h/h_{wb}). \qquad (4)$$

The energy available for driving cliff retreat, E_{cliff}, is the original energy in the far field wave climate, E_o, reduced by the spatial integral of the dissipation rate along its

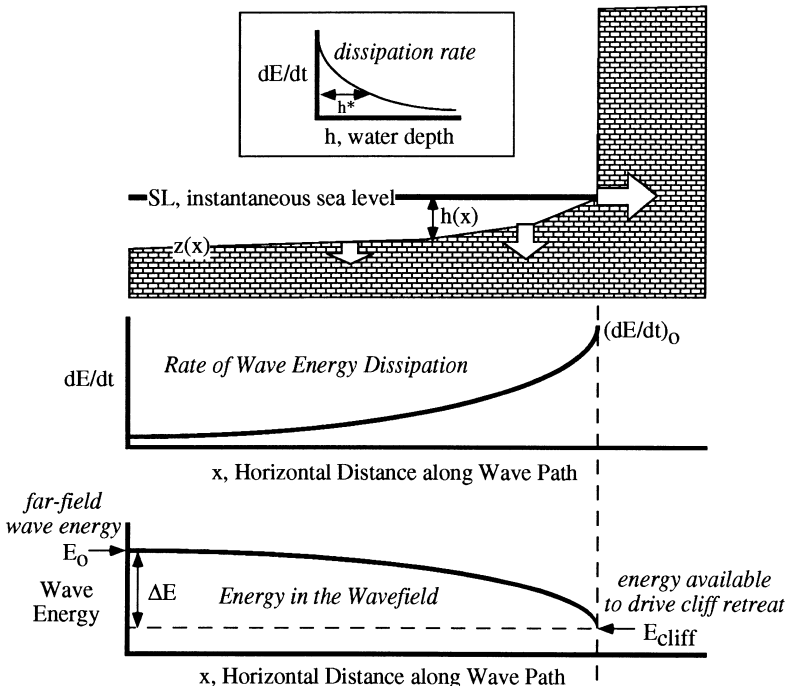

Fig. 4. Rules governing the spatial distribution of erosion rates (arrows) given the instantaneous sea-level, SL, and the water depth profile, $h(x)$. Sea bed erosion rate (arrows) tends as the rate of dissipation of wave energy, which decays exponentially with water depth, h (top box; eqn 2). The water depth profile therefore dictates the spatial pattern of dissipation rate and hence of erosion rate (first plot). The energy remaining in the wave (bottom plot) declines slowly at first and most rapidly nearest the shore, to leave $E_o - \Delta E = E_{cliff}$ at the cliff edge. Some fraction of the energy remaining at the cliff base, all of which is dissipated in littoral processes, is then used to drive cliff retreat.

path (Fig. 4), or $E_{cliff} = E_o - \Delta E$, where

$$\Delta E = \int_0^\infty (dE/dx)\, dx. \quad (5)$$

For the simplest case of a planar shelf with a uniform slope of θ, i.e. $h = x \sin(\theta)$, this integral becomes

$$\Delta E = (dE/dt)_o 4h_{wb}/V \sin(\theta). \quad (6)$$

The horizontal length scale

$$x^* = 4h_{wb}/\sin(\theta) \quad (7)$$

corresponds to the length of shelf over which most of the wave energy is dissipated. This expression merely codifies the fact that regions with extensive shallow shelves should allow less energy to the cliff to drive erosion.

In the more general case of variably sloped sea floors, we assess the dissipation of energy along the wave path incrementally. The rate of energy dissipation at any point, x, on the sea floor is converted to erosion of the sea floor using Eq. (2). In the numerical experiments to follow, we assume that the rate of retreat of the cliff into the landmass is linearly proportional to the wave energy remaining at the instantaneous shoreline:

$$(dx/dt)_{cliff} = \beta_{cliff} E_{cliff}. \quad (8)$$

This assumes that all of the remaining energy in the waves is dissipated at the shoreline. The constant β_{cliff} folds together the fraction of this energy that is available for erosion, and the resistance of the local rock to erosion. On the Santa Cruz coastline, it is clear that the cliff material produced by failures of the cliffs rapidly disintegrates on the beach and is efficiently carried away by longshore processes. We therefore assume that cliff retreat rate is not limited by the need to transport this material, and is therefore independent of cliff height.

TERRACE GENERATION EXPERIMENTS

We illustrate the terrace generation problem with a simple 1-D case. The initial landmass is taken to be a homocline with a prescribed seaward slope of 5°. Tectonic uplift is uniform at a rate of 1 mm yr^{-1}, which is somewhat higher than the 0.3 mm yr^{-1} documented for the Santa Cruz coastline (Bradley & Griggs, 1976; Valensise & Ward, 1991; Anderson & Menking, 1994). Simulations with this higher rate better illustrate the complexity of the problem. We present two cases, one with dissipation, the other without (Fig. 5). While both simulations generate a staircase of terrace flats separated by sea cliffs, the flights of terraces differ in detail. In the case of no dissipation, the distance the sea cliff retreats into the landmass is simply proportional to the duration of the sea-level rise. The wave-cut bench profile therefore maps almost perfectly into the sea-level curve (Fig. 5a). The sequence of highstands and durations of periods of sea-level rise then sets the widths of the remaining terrace platforms. It follows that a long-duration sea-level highstand can obliterate an older platform. In this simulation, for example, the 5e terrace is lost.

Dissipation lessens the likelihood of such a demise of an older platform, and generates a more complete set of terraces. In this case, as the wave-cut platform extends through the course of a relative sea-level highstand, it reduces the ability of subsequent waves to reach the sea cliff with significant energy, thereby lowering the rate of retreat (Fig. 6). Dissipation forces a dramatic departure

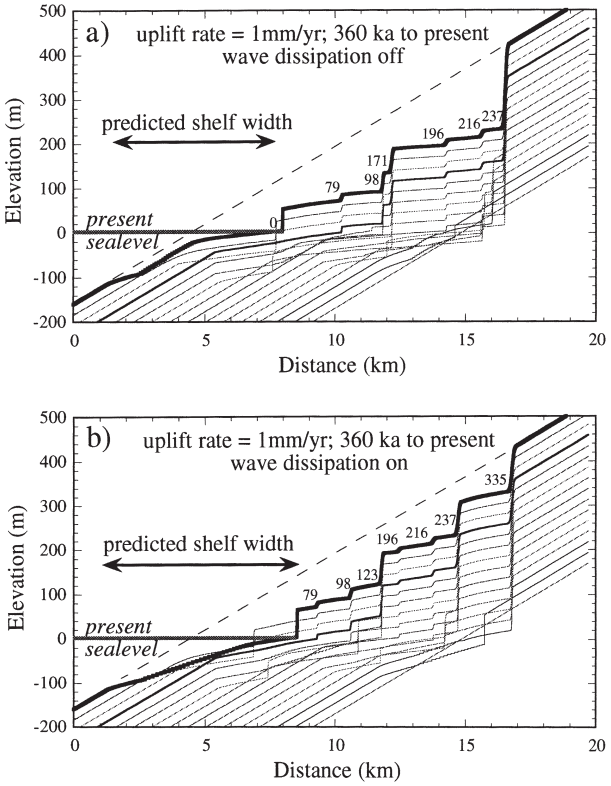

Fig. 5. Simulated terraces and associated sea cliffs over 360 ka model run, differing only in that the dissipation is turned off in (a) and left on in (b). The uplift in each case is held steady and uniform at 1 mm yr^{-1}. These simulations serve to illustrate the subtle role of dissipation in the resulting set of preserved cliffs. The bedrock pattern is stamped every 24 ka. Ages of cliffs are noted in ka. When dissipation is off, the cliff retreats at a constant rate of 0.4 m yr^{-1}. When turned on, cliff retreat is greatly modulated by the instantaneous shape of the sea floor (Fig. 6). The predicted width of the wave-bevelled portion of the continental shelf is noted. The bevelled portion of the continental shelf is wider when dissipation is turned on, and has a significantly less prominent bulge in the offshore profile. Note that the predicted width of the wave-cut platform generated since the last deglaciation ($\approx$18 ka) is significantly wider when wave energy dissipation is neglected.

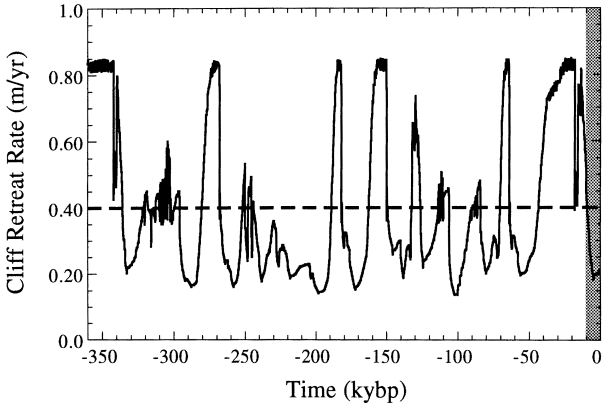

Fig. 6. Sea cliff retreat rate history under conditions of wave dissipation. Mean rate of 0.4 m yr^{-1} is dictated by the model inputs to correspond to the no-dissipation case. A roughly four-fold modulation of cliff retreat rate results for the particular chosen dissipation constants, with markedly greater retreat rates at sea-level lowstands than at highstands. The most recent highstand is shown by grey shading. Note the Holocene decline of the cliff retreat rate as the modern platform has extended.

from the mean rate of cliff retreat, which we have set to 0.4 m yr^{-1} to correspond to representative rates along the Santa Cruz coastline (Best & Griggs, 1991). One can see, for instance, the four-fold reduction in the cliff retreat rate through the post-LGM increase in sea-level as the waves are made to travel across the broadening platform (Figs 5b and 6). This effect therefore protects older platforms, and (interestingly) reduces the importance of highstand duration in setting the terrace sequence; most of the geomorphic work is done early in the highstand. As the defeat of one platform by another is difficult to see in the series of profiles shown in Fig. 5, we show in Fig. 7(a) time series of cliff positions with arrows denoting the positions of cliff edges that survive through to the present. The difference is most marked in the predicted preservation of the $\approx$125-ka highstands.

Interestingly, for the initial conditions used in the calculations, and the rates of cliff retreat we have imposed, the width of the resulting wave-cut platform is at least several kilometres (Fig. 5). Its lower limit is the lower bound of wave-cutting attack, which is dictated by the lowest sea-level lowstands of $\approx$120–150 m below present sea-level. Little information exists on the outer margin of the shelf that would allow further assessment of the lower set of terraces to be expected in such a scenario. Locally, coarse beach sands have been reported at that bathymetric level in the margins of Monterey Bay (J. Tait and J. Revenaugh, personal communication, 1997). The pattern of terrace survival is significantly higher for highstand vs. lowstand terraces. While uplift favours preservation of last highstand platforms by taking the inner edge out of the band of climatically driven sea-levels, it simultaneously and for the same reasons brings rock into which lowstand platforms had been etched into the teeth of the wave-cutting saw.

DEGRADATION OF PALAEO-CLIFFS

Modern sea cliffs near Santa Cruz slope at 80–90°. The shoreline is deeply crenulated, with pocket beaches and coves ornamenting the coastline, separated by jutting headlands. We do not pretend to model this detail, which would require a 2-D planform model and all its attendant attention to the details of wave refraction. Instead, we focus on the 1-D cross-section through the coastline. The initial condition therefore for any particular terrace is a nearly vertical cliff, topped with a terrace sand sequence several metres thick from a prior regression of the sea. This problem has been addressed by many previous workers, most prominently Hanks *et al.* (1984), who were the first to attempt to use the degraded cliff profiles to date the various platforms in the Santa Cruz area (see also Crittenden & Muhs, 1986). Most recently,

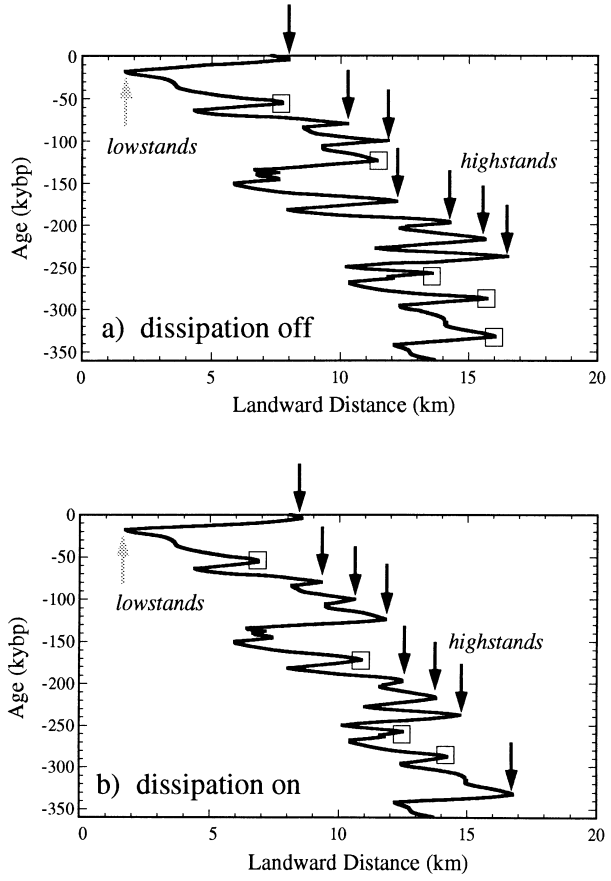

Fig. 7. Coastline position history from the two models depicted in Fig. 5. The arrows depict preserved sea-level lowstand (grey arrow) and highstand (black arrows) terrace knicks in the final landscape for dissipation on case (a) and dissipation off cases (b). To first order, these diagrams look like canted versions of the $\delta^{18}O$ curve. The slant of each diagram is dictated by the crustal uplift rate. Boxes denote sea cliffs that existed on the landscape for some time, but have been removed by the further landward retreat of subsequent sea cliffs. It is in the pattern of the boxes and arrows that the two cases differ. For instance, the 5e sea cliff ($\approx$125 ka) is preserved in the case with dissipation (b), while it is destroyed in the no-dissipation case (a). Similarly, the 330-ka cliff is retained when dissipation prevents the 250-ka cliff from retreating so far into the landmass. Note also that while many lowstand knicks are generated, only one is likely to be preserved at any time. At present, this would be that from the last glacial maximum lowstand.

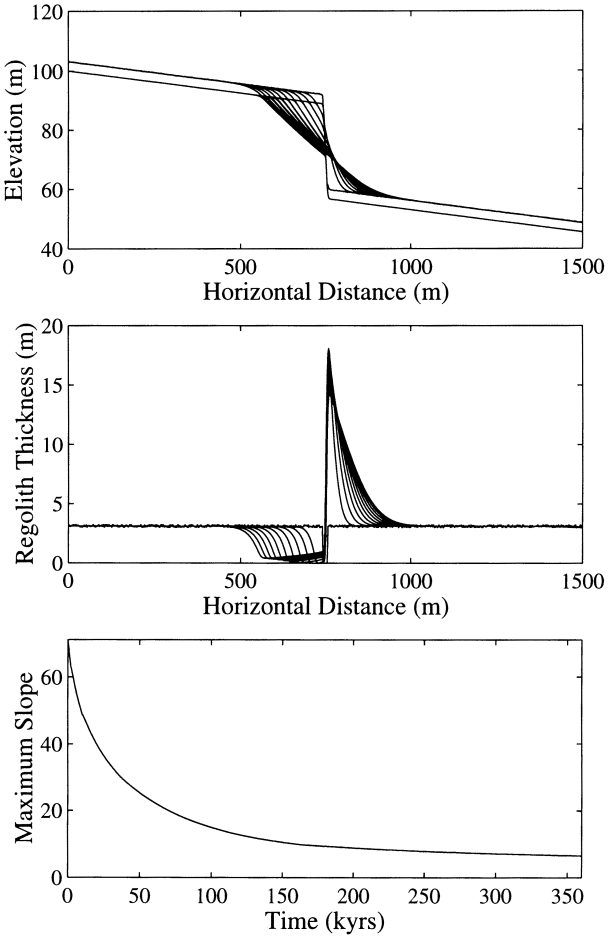

Fig. 8. Simulations of cliff degradation covering 360 ka. Two 750-m-wide terrace platforms sloping at 1.5° are separated by a 30-m sea cliff. As the simulation begins, the cliff angle is 70°, and each platform is topped by 3 m of terrace sands with initial random microtopography of the order of 25 cm. The profiles of the bedrock–regolith interface, and the top of the regolith are shown in 10 time stamps (36 ka apart) in the top panel, while the regolith thickness profile is depicted in the second panel. Note the decline in the maximum slope through time, shown in the bottom panel, and the shallow regolith at the edge of the terrace flat throughout the simulation. Following the work of Rosenbloom & Anderson (1994), this emphasizes the departures from the pure diffusion case, in which the curvature at top and base of the profile would be identical, and points out the potential value in obtaining regolith thickness profiles in such landscapes.

Rosenbloom & Anderson (1994) provide a more detailed model of cliff evolution that differs from that of Hanks and others primarily in that it includes explicitly the role of generation of regolith that is a prerequisite for the movement of material downslope. The downslope movement was then modelled as a diffusive process, following Hanks *et al.* (1984) and many others. The process involved is presently dominated by the actions of rodents (Black & Montgomery, 1991; Rosenbloom & Anderson, 1994), which efficiently move colluvium preferentially in the downslope direction, and coincidentally allow other surface processes such as rainsplash to diffuse their burrowings yet further. This is a system similar to the one described by Jyotsna & Haff (1997) in which two processes operating on two length scales can drive diffusional decay of hillslopes. In many cases, rodents appear to be the rate-limiting agents of transportation.

Cliffs decay through time (Fig. 8). To first order, the cliff degrades diffusively. However, while the highly mobile terrace sands rapidly relax to a much lower slope, the retreat of the bedrock cliff itself is weathering-limited, and the cliff retains high curvature for many tens of thousands of years, efficiently flushing any sediment that is removed from the terrace flat above. Colluvium accumulates on the next lower terrace, mantling the

terrace sands. In contrast to a purely diffusive system, the palaeocliff retains an asymmetry, showing a highly curved crest, and a much straighter toe. The regolith profile thins from its maximum over the terrace platform to a minimum very near the crest of the palaeocliff. The predicted profile then thickens slightly before the edge of the colluvial wedge (Fig. 8). Despite these details, the cliff degrades monotonically through time, most rapidly at first, the rate decaying through time. The model fits to detailed topographic profiles along the Santa Cruz coastline presented by Rosenbloom & Anderson (1994) imply that the rate of production of regolith from the local bedrock, a siliceous mudstone, is at least 0.1 mm yr^{-1}, and that the diffusivity of the material once freed from bedrock is roughly 11 m^2 ky^{-1}. This is very close to the value obtained by Hanks *et al.* (1984). The rate of bedrock transformation into regolith is similar to that documented by atmospherically produced ^{10}Be inventories in clay hillslopes of the eastern San Francisco Bay area (McKean *et al.*, 1993), and to that documented in other vegetated California settings using *in situ* produced ^{10}Be (Heimsath *et al.*, 1997), and it is significantly higher than that documented on bare bedrock outcrops in arid and alpine settings (Bierman, 1994; Small *et al.*, 1997).

Landsliding is likely to be a dominant mechanism for sea cliff decay soon after abandonment, particularly by rockfall early on and deep-seated or rotational slumping thereafter. In summary, cliffs decay rapidly at first, possibly by landsliding, and more slowly thereafter, dominantly by diffusional action of rodents. In a purely diffusive system, the maximum slope angle of a cliff declines at a rate proportional to the square root of age (Hanks *et al.*, 1984). With diffusivities of 11 m^2 kyr^{-1}, maximum slope angles of cliffs starting at 70° will still be of the order of 10° after roughly 1 million years. Indeed, small remnants of these palaeocliffs can be easily recognized in the landscape, even when they now form essentially only local shoulders in narrow interfluves.

STREAM CHANNEL GENERATION AND INCISION

A rising landmass will be attacked by a set of streams, which both etch into the rock and transport debris delivered to their margins by adjacent hillslopes. Base-level for each stream will be set at its intersection with the instantaneous sea-level, which fluctuates with an amplitude of 120–130 m. While there is considerable debate about how to model bedrock incision by streams (e.g. Howard & Kerby, 1983; Seidl & Dietrich, 1992; Hancock *et al.*, 1998), most workers fall back upon traditional arguments that the incision rate will be dictated by the local stream power, usually taken as the product of the local discharge and the local stream channel slope. This approach was used by Rosenbloom & Anderson (1994) in their treatment of terrace-crossing channels in the Santa Cruz landscape.

The more difficult problem of how to generate a stream pattern on a virgin landscape freshly emerged from the sea was not treated by Rosenbloom & Anderson (1994). Later, 2-D planform landscape evolution models attempt to explore this problem (Densmore *et al.*, 1998). In a series of numerical experiments, described in Densmore *et al.* (1998) and Ellis *et al.* (1999), we imposed a threshold stream power, essentially a slope–area product threshold akin to that found by Montgomery & Dietrich (1988) in localizing the channel head in numerous landscapes. As the channel head incised, it enhanced the local channel head slope through hillslope processes, allowing advance of the channel head. We found a very interesting behaviour, reflecting a fierce competition for water resources. The palaeocliffs became ornamented with young budding channels, which initially might have very similar drainage areas, given the planar nature of the terraced flat they were draining. As the channel heads advanced, those with slightly more drainage area advanced more rapidly. These then increased the slopes of the interfluve toward them, caused slight retreats of divides, and thereby captured some fraction of the drainage area of the adjacent channel. The result is that an initially healthy channel could be defeated by capture of its drainage area by an adjacent channel. That there will be slight differences in the initial drainage areas is an unavoidable consequence of even the slightest randomness of the initial topography. One would therefore predict that some fraction of the initial drainages will die, which is in fact the case. Many instances of channel death are seen along the coast north of Santa Cruz (Fig. 1). It is also possible for a channel to defeat itself through reduction of its initial very steep slope (Fig. 9a). Here the channel has sufficient drainage area above the steep initial scarp to power its incision in the early years. If, however, the product of discharge and local slope is only slightly more than that necessary to cause incision, then rapid decline in channel slope upon the headward march of the channel head may result in eventual reduction of all points in the catchment to below the channel head threshold (Fig. 9b). The channel form is then relict, and may remain as an indentation in the landscape for long periods of time as it is slowly filled in by colluvial processes. These dead channels serve to ornament and fragment the terrace platforms.

The initial spacing of the channels is thus established by the threshold stream power, which sets the framework for the ensuing channel competition. As the channel network evolves toward a stable configuration, however, the important controls on channel spacing become the width and relief of the coastal topography, which are ultimately set by the tectonic uplift pattern and the rate of base-level change (e.g. Hovius, 1996; Talling *et al.*, 1997).

The largest of the channels, those that become the through-going channels draining the rising massif, are powerful enough to incise through the palaeocliffs. It is these that are responsible for most efficiently carving up the terraces, which lose their spatial continuity through time. The long profiles of these throughgoing streams will retain for some time the signature of the complex fluctuations in base-level that the stream has encountered

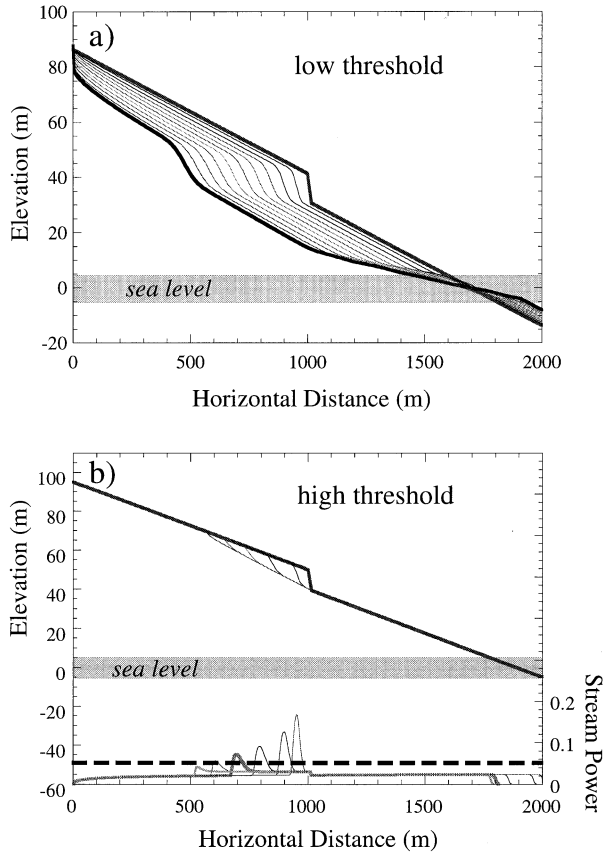

Fig. 9. Simulations of channel incision, with low (a) and high (b) threshold relative to the available stream power. Initial conditions are identical in the two simulations. Again, instantaneous profiles are stamped at equal time intervals. While stream power remains high relative to the channel incision threshold in the top simulation, driving continued incision and retreat of knickpoints into the profile, the stream in the lower panel manages to defeat itself. Here the channel slope has declined until no point on the channel has a stream power above that necessary to drive incision (denoted by dashed line).

through many glacial cycles (Rosenbloom & Anderson, 1994). As base-level varies vertically, the point at which this boundary condition is applied to the landscape migrates horizontally. In some cases, this results in the landward migration of knickpoints corresponding to sea cliff retreat at rates greater than the rates at which the stream can incise (Fig. 9b; see also Rosenbloom & Anderson, 1994). The larger the stream, the more rapidly it responds to base-level changes imposed by sea-level fluctuations. For the larger streams in the Santa Cruz area, the response is such that the bedrock of the channel is below present sea-level for >1 km inland from the sea. These bedrock channels match corresponding sand-filled channels on the sea floor, reflecting incision during the LGM. The near-coast reaches of these streams were alluviated during the Holocene sea-level rise (Fig. 1). In addition, the consequence of this efficient incision on the degradation of the terraced fringe of the landscape is that the local base-level for the channel-bounding hillslopes is well approximated by sea-level.

MASS WASTING ADJACENT TO INCISING CHANNELS

Channel incision drives down the boundaries of adjoining slopes. This increases the steepness of valley sides, making the slopes more susceptible to failure. Given the depths of incision of the major streams into the terraced landscape, it is unlikely that the slopes will remain vertical for long, much as it is unlikely that palaeo-sea cliffs remain near-vertical. Many of the valley slopes adjacent to the channels in the Santa Cruz landscape are $\approx 30^\circ$, and are by far the steepest slopes in the landscape but for the youngest palaeo-sea cliffs. Rather than model the effects of individual landslides, as we have done elsewhere (Densmore *et al.*, 1998; Ellis *et al.*, 1999), we simplify the problem by appealing to a simple geometric argument. If, over long periods, occasional landslides maintain hillslope angles close to the angle of slope stability, α, as the channel incises into bedrock, then the forget time, T, necessary to remove a terrace platform (the interfluve between two incising streams) depends upon the incision rate of the streams, the along-shore spacing between major streams capable of incising through the terraced landscape, L, and the hillslope angle, α (Fig. 10):

$$T = H/(\mathrm{d}H/\mathrm{d}t) \approx (L/2)\ (\tan \alpha)/U. \quad (9)$$

Here H is the local height of the terrace surface above the bounding stream. As argued above, the master streams will efficiently keep pace with sea-level. If sea-level were to remain constant, then the incision rate may be replaced by the uplift rate, U. For the Santa Cruz terraced fringe, with spacing between major streams of the order of 500 m, an uplift rate of 0.3 mm yr^{-1}, and a bedrock failure angle of the order of 30°, this implies a forget time of ≈ 500 ka.

We fully recognize that this treatment of channel incision oversimplifies the problem immensely. The most egregious omission is that the stream systems are not single trunks, but ramify significantly into networks upstream (Figs 1 and 11). As the tributaries etch into the landscape, they drive retreat of the bounding hillslopes, further dismembering the terrace platform. This problem is both nonlinear and site-specific, nonlinear in that the retreat rate of a channel bud depends upon the upstream contributing area, which diminishes as the channel advances; and site-specific because the size and shape of the contributing basin become important. We note also that the most significant eradication of terraces via fluvial and coupled hillslope processes should take place, all else being equal, during low sea-levels, when knickpoint migration drives rapid incision, enhancing both slope failure and channel head retreat. The problem is complicated by the fact that this increased stream gradient must access the landmass inland of the old sea cliff to result in significant enhancement of terrace degradation. Whether this occurs depends upon the width of the shelf across which the base-level effects

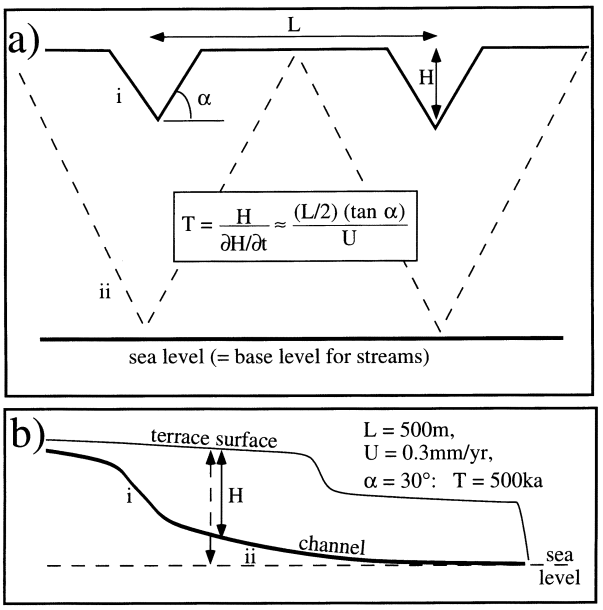

Fig. 10. Schematic of channel wall retreat into a terrace platform forced by incision of the bounding streams. As a throughgoing large-power channel incises downward into the rock mass (b; see also Fig. 9a), it deepens relative to the terrace surface above it. The local distance between the channel and the terrace surface, H, grows through time as the channel incises, such that a cross-section at early time (i) transforms into a later cross-section (ii). This second section is shown in (a) with its maximum relief, having eliminated the terrace platform flat. For very large streams capable of keeping pace with sea-level, the rock uplift rate, U, is a good surrogate for the incision rate. If the bedrock slopes bounding the channel are controlled largely by rock strength, such that they may be assumed to have slopes of roughly equal angles (say $\alpha \approx 30°$), the deepening of the channel translates linearly into a reduction of the interfluve width. The time-scale for removal of the terrace flat (the memory time for terraces in a landscape) is therefore simply dictated by the initial spacing between throughgoing drainages, L, the rock strength (through α) and the uplift rate, U. For parameters typical of the Santa Cruz coastline, this predicts a memory time of roughly 500 ka.

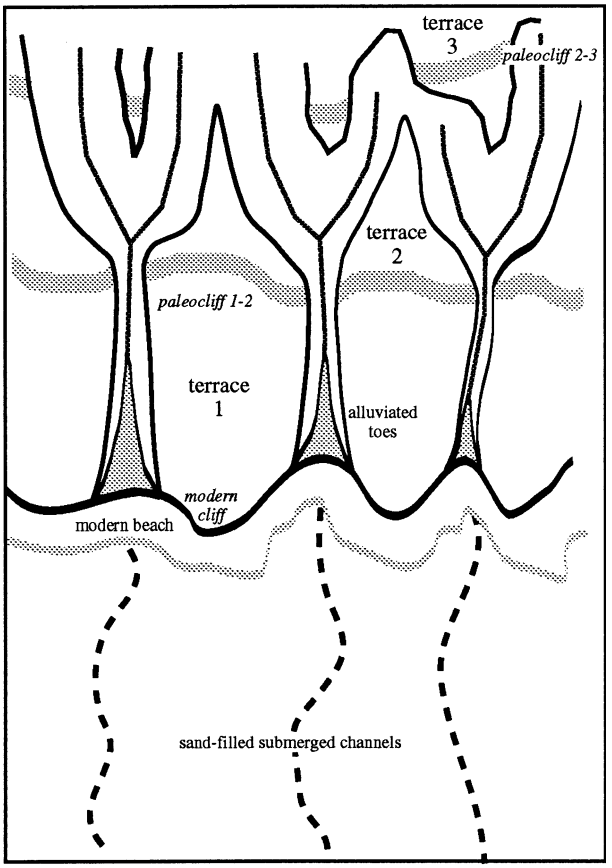

Fig. 11. Detailed schematic of the terraced fringe of a coastal landscape, showing the modern sea cliff; the beach sands locally mantling and obscuring the offshore extension of the streams into sand-filled troughs in the modern wave-cut platform; a sequence of three marine terraces becoming more dissected landward by a widening of channel walls as the stream both ramifies landward and deepens into the rock mass; and the alluviated toes of the modern streams (grey flared patches).

must propagate, the duration of the lowstand, and the efficiency of channel incision, itself dependent upon basin characteristics and precipitation. Rather than embark on the fuller but less general modelling necessary to explore these effects, we merely note that our calculations of forget time should therefore yield minimum estimates.

DISCUSSION

It has long been known that both erosional and depositional systems are imperfect recorders of past events. In fact, this is part of the charm and attraction of the geological sciences, the challenge to solve the mysteries with most of the pages missing. One of the first attempts to formalize this effect was the novel treatment of moraine survival (Gibbons *et al.*, 1984). They showed that for every 20 moraines built by random lengths of glacial advance, roughly four would be left in the record, as long glaciers obliterate the moraines of all older, shorter ones. In this paper, we have described an analogous system in which younger marine wave-cut platforms can obliterate the record of older ones. We have noted in Fig. 7 those terrace edges that survive (arrows) and those that are ultimately destroyed (boxes) in the marine terraced landscape. The pattern of survival depends upon many of the variables in the problem, including the history of sea-level and of the wave climate (in all of our simulations to date we have not varied the wave climate), and the erodibility of the substrate. The pattern also depends in a complex way on the uplift pattern in that this will affect the water depths over the shelf, the pattern of which plays an important role in the dissipation of wave energy. Finally, once formed, a terrace faces yet other destructive forces of terrestrial geomorphology. The oldest terraces in the Santa Cruz areas, for example, are only about 500 ka, despite the fact that the terrace generation mechanism has likely been in place for the entire Quaternary. Workers in other disciplines in geology have had to address other examples of the incompleteness

of the record. For example, Paola & Borgman (1991) worried about what fraction of a channel depth would be left in the record, a necessary value for calculating palaeo-discharges. Sadler (1981) addressed the question of what fraction of the time represented by some stratigraphic column resulting from slowly accumulating deposit in the face of fluctuating deposition/erosion rates was actually recorded.

What is in common among these phenomena is the one-sided nature of the processes, and the stochastic nature of the forcing mechanism. Moraines result from a glacier that sweeps up and down a valley, stratigraphy is generated by processes that either erode into or deposit upon the land surface, and fluvial and marine terraces are generated by lateral incision into a landmass. All of these processes are therefore one-sided: the forcing comes from one direction. In the marine terrace problem, as a sloping landmass rises, it drives a long-term relative regression of the sea. It is this drift of the system that promotes preservation of terraces (reflected by the slope of the sea–land intersection history plots in Fig. 7). This signal is modulated by sea-level changes, as imprinted by the wave-driven incision of the sea cliff. The lower the slope of the landmass rising from the sea, the faster this regression, and the more likely the preservation of (and the broader) the resulting terrace platforms. The system is different from the morainal one in that it has this net drift, and in that there is the potential of a complete removal of the terrace cliff by erosional processes. Were there no drift (rock uplift = 0), only one subaerial terrace could be recorded within the last few hundreds of thousands of years, corresponding to the 5e highstand about 6 m above present sea-level. Note that long-term subsidence, on the other hand, might result in the recording of a series of submerged terraces corresponding to the sea-level lowstands (e.g. Ludwig *et al.*, 1991). At present, on a rising landmass, we would expect the bathymetry to reflect only one lowstand (Fig. 7), from the last glacial maximum; note in Fig. 5 that the record of this lowstand is not a distinct knick in the topography, but rather a more subtle change in slope.

Terraces are distinctive landscape features because they are planar, low-relief surfaces; even dissected scraps of terraces can still be recognized as benches aligned at a relatively constant height. While one could presumably define terraces on the basis of discrete spikes in a hypsometric derivative plot, we note that the human eye is remarkably acute at discerning linear or planar features, and thus serves as an adequate tool. We have seen that channel processes ultimately set the time-scale for the erasure of these planar features from a landscape (Figs 1 and 11). For the Santa Cruz landscape, it is reasonable to expect terraces of 500 ka ages to be discernible in the landscape. As far as is known of the terrace ages (e.g. Bradley & Griggs, 1976; Kennedy *et al.*, 1982; Lajoie *et al.*, 1986; Muhs *et al.*, 1994), this appears to be roughly the case. In detail, however, there appear to be lithologically controlled variations in the preservation, even along this 40 km of coastline. In the Aptos area studied by Alexander (1953), only three platforms are recognized, the third only patchily. North of Santa Cruz, however, five distinct platforms are recognized (Bradley & Griggs, 1976). While the uplift rates for these two areas are within 10–20% of each other (Anderson & Menking, 1994), the difference lies primarily in the lithology. The Aptos area is dominated by weaker Plio-Pleistocene sandstones of the Purisima formation, while the north coast is dominated by the stronger, finer-grained siliceous Miocene Santa Cruz mudstone. The chief effects of the weaker lithology lie in the enhancement of the efficiency of coastal cliff incision, and in the lower spacing between throughgoing channels, reflecting presumably the lower stream power necessary to incite channellization of the landscape. In the Aptos area, the enhanced efficiency of cliff retreat one might expect from the lithology is now countered by the geometry of the coastline, which has progressively become more sheltered from the wave attack through deepening of the Monterey Bay embayment. While we cannot handle this planview complexity in our 1-D models, it is certainly an excellent target for further research.

The marine terraced fringe of a landscape, taken as a whole, can be viewed as a steady-state feature if the uplift mechanisms have been operating for long enough to pass a rock parcel entirely through this benched boundary layer. While the details of the terrace spacing will vary from one glacial cycle to the next, the basic look of the landscape – with benches near the sea and none above some altitude or some distance inland – should remain constant. For the central California example we have used for illustration, the memory time-scale involved is of the order of 500 ka, and the length scale is on the order of ≤ 10 km.

An interesting apparent exception to this basic model comes from terraced sites that for one or another reason lack the larger drainage areas. Terraces developed on islands (e.g. San Clemente Island, California (Muhs, 1983), San Nicolas Island, California (Muhs, 1985) and Hawaii (Ludwig *et al.*, 1992)) and on relatively narrow peninsulas (e.g. Baja California (Rockwell *et al.*, 1989)) appear to be better preserved than those fringing a larger landmass. In these settings the maximum lengths of the drainages are roughly the half-width of the island or peninsula. This has the effect of limiting the stream power available to drive incision, which ultimately limits dissection of the landscape. For similar reasons, a very arid climate can yield long-lived terraces, as is found along the Peruvian coast (Hsu, 1992).

We note that the model of terrace generation we have presented is the simplest possible 1-D model. The only wrinkle it possesses is the incorporation of wave energy dissipation. While even this inclusion yields new insight into the generation of a sequence of terraces, there are several opportunities to advance this model significantly. First, the far field wave energy is held constant in the present model. In reality, most coastal cliff retreat takes

place in discrete storm events, the most efficient work taking place during a conspiracy of high tides, storm surge and depleted sandy beaches (which serve as local dissipators of wave energy). Given that storm frequency, magnitude and even temporal spacing all likely vary within the glacial–interglacial climate cycle, driven by variations in both global winds and sea surface temperatures, we would expect that the wave forcing of the system would be coupled to the sea-level cycle. To the degree that the storminess is linked to the hydrographic variables, this will also drive significant variation in the forcing of the incision of the coastal streams. Second, we do not address the issue of event sequencing. In our model, each incremental time slice yields the same far field wave energy, effectively bypassing all climatic variations. In addition, each packet of wave energy that does make it to a cliff can perform the same amount of work on the cliff. This latter assumption therefore ignores the effects of beaches as dissipators of energy. As witnessed during 1998 and other El Niño events along California coasts, once waves have removed the beach dissipators, coastal erosion takes place more efficiently. Because a cliff is more vulnerable to late season storms than to early storms, the event sequence becomes important. Third, rocky coasts are not straight, but have significant headlands and coves. In order to attack this portion of the problem, one would have to model the coastal retreat in planview as well. This would necessarily entail treatment of the wave refraction problem. Such an investigation would be enriched in that the farfield forcing of the wave field could be made directional, allowing incorporation of the dominant swell directions and their variation with climate. Detailed coastal topography such as pocket coves and headlands become constraints on the problem. We view all of these as strong targets of research opportunity.

ACKNOWLEDGEMENTS

This work was accomplished with the aid of grants to R.S.A. and M.A.E. from NASA's Surface Change Program. This is CERI contribution number 349, and Institute for Tectonics Contribution number 385. We thank Greg Hancock for editorial comments on an early draft of the manuscript, Chris Paola, John Wehmiller and especially Dan Muhs for very helpful reviews, and Doug Burbank for careful editing of the final version.

List of Symbols

Symbol	Definition	Units
E_o	Far field wave energy	Energy, E
dE/dx	Spatial gradient in energy dissipation	E/L
dE/dt	Temporal gradient in energy dissipation	E/T
h	Water depth ($SL-z$)	L
h^*	Length scale for decay of dissipation rate with water depth	L
h_{wb}	Wave base, depth at which waves do not feel bottom	L
H	Depth of channel incision into terrace surface	L
L	Channel spacing	L
SL	Sea-level	L
t	Time	T
U	Rock uplift rate	L/T
V	Wave speed normal to the coastline	L/T
x	Distance from instantaneous shoreline	L
x^*	Horizontal length scale for decay of wave energy	L
z	Elevation of topographic surface	L
α	Hill slope adjacent to a channel	None
β	Erosion constant for sea floor	L/E
β	Cliff erosion constant for sea cliff	L/E–T
λ	Wave length	L
θ	Slope of sea floor	None

REFERENCES

Alexander, C.S. (1953) The marine and stream terraces of the Capitola-Watsonville area. *Univ. Calif. Publs. Geog.*, **10,** 1–44.

Anderson, R.S. & Menking, K.M. (1994) The Santa Cruz marine terraces: evidence for two coseismic uplift mechanisms. *Geol. Soc. Am. Bull.*, **106,** 649–664.

Bard, E., Hamelin, B. & Fairbanks, R.G. (1990) U-Th ages obtained by mass spectrometry in corals from Barbados: sea level during the past 130 000 years. *Nature*, **346,** 456–458.

Best, T.C. & Griggs, G.B. (1991) A sediment budget for the Santa Cruz littoral cell, California. In: *From Shoreline to Abyss, Spec. Publishers. Soc. Econ. Paleontol. Mineral.*, **46,** 35–50.

Bierman, P.R. (1994) Using in situ produced cosmogenic isotopes to estimate rates of landscape evolution: a review from the geomorphic perspective. *J. Geophys. Res.*, **99,** 13885–13896.

Black, T.A. & Montgomery, D.R. (1991) Sediment transport by burrowing mammals, Marin County, California. *Earth Surf. Processes Landforms*, **16,** 163–172.

Bradley, W.C. (1957) The origin of marine-terrace deposits in the Santa Cruz area, California. *Geol. Soc. Am. Bull.*, **68,** 421–444.

Bradley, W.C. & Griggs, G.B. (1976) Form, genesis, and deformation of central California wave-cut platforms. *Geol. Soc. Am. Bull.*, **87,** 433–449.

Chappell, J.M. & Shackleton, N.J. (1986) Oxygen isotopes and sea level. *Nature*, **324,** 137.

Cinque, A., De Pippo, T. & Romano, P. (1995) Coastal slope terracing and relative sea level changes; deductions based on computer simulations. *Earth Surf. Processes Landforms*, **20,** 87–103.

Crittenden, R.C. & Muhs, D.R. (1986) Cliff height and slope angle relationships in a chronosequence of marine terraces, San Clemente, California. *Z. Geomorphol.*, **30,** 291–301.

Densmore, A.L., Ellis, M.E. & Anderson, R.S. (1998) Landsliding and the evolution of normal fault-bounded mountains. *J. Geophys. Res.*, **103,** 15203–15219.

Ellis, M.A., Densmore, A.L. & Anderson, R.S. (1999)

Evolution of mountainous topography in the Basin and Range Province. *J. Geophys. Res.*

Fairbanks, R.G. (1989) A 17 000-year glacio-eustatic sea level record: Influence of glacial melting rates on the Younger Dryas event and deep–ocean circulation. *Nature,* **342,** 637–642.

Gibbons, A.B., Megeath, J.D. & Pierce, K.L. (1984) Probability of moraine survival in a succession of glacial advances. *Geology*, **12,** 327–330.

Hancock, G.S., Anderson, R.S. & Whipple, K.X. (1998) Beyond power: Bedrock river incision process and form. In: *Rivers Over Rock: Fluvial Processes in Bedrock Channels* (Ed. by K. Tinkler & E.E. Wohl), pp. 35–60. AGU Press.

Hanks, T.C., Bucknam, R.C., Lajoie, K.R. & Wallace, R.E. (1984) Modification of wave-cut and faulting-controlled landforms. *J. Geophys. Res.*, **89,** 5771–5790.

Heimsath, A.M., Dietrich, W.E., Nishiizumi, K. & Finkel, R.C. (1997) The soil production function and landscape equilibrium. *Nature*, **388,** 358–361.

Hovius, N. (1996) Regular spacing of drainage outlets from linear mountain belts. *Basin Res.*, **8,** 29–44.

Howard, A.D. & Kerby, G. (1983) Channel changes in badlands. *Geol. Soc. Am. Bull.*, **94,** 739–752.

Hsu, J.T. (1992) Quaternary uplift of the Peruvian coast related to the subduction of the Nazca Ridge: 13.5–15.6 degrees latitude. *Quat. Int.*, **15/16,** 87–97.

Imbrie, *et al.* (1984) The orbital theory of Pleistocene climate: support from a revised chronology of the marine d18O record. In: *Milankovitch and Climate* (Ed. by A. Berger *et al.*), pp. 269–305. D. Reidel, Dordrecht, Netherlands.

Jyotsna, R. & Haff, P.K. (1997) Microtopopgraphy as an indicator of modern hillslope diffusivity in arid terrain. *Geology*, **25,** 695–698.

Kennedy, G.L., Lajoie, K.R. & Wehmiller, J.F. (1982) Aminostratigraphy and faunal correlations of late Quaternary marine terraces, pacific coast, U.S.A. *Nature*, **299,** 545–547.

Lajoie, K.R., Ponti, D.J., Powell, C.L., Mathieson, S.A. & Sarna-Wojcicki, A.M. (1986) Emergent marine strandlines and associated sediments, coastal California; A record of Quaternary sea level fluctuations, vertical tectonic movements, climatic changes, and coastal processes. In: *The Geology of North America, Vol. K-2, Quaternary Nonglacial Geology: Conterminous U.S.* (Ed. by R.B. Morrison), pp. 190–214.

Ludwig, K.R., Muhs, D.R., Simmons, K.R. & Moore, J.G. (1991) Sr-isotope record of Quaternary marine terraces on the California coast and Hawaii. *Quat. Res.*, **37,** 267–280.

Ludwig, K.R., Szabo, B.J., Moore, J.G. & Simmons, K.R. (1992) Crustal subsidence rate off Hawaii determined from 234U/238U ages of drowned coral reefs. *Geology*, **19,** 171–174.

McKean, J.A., Dietrich, W.E., Finkel, R.C., Southon, J.C. & Caffee, M.W. (1993) Quantification of soil production and downslope creep rates from cosmogenic ^{10}Be accumulations on a hillslope profile. *Geology*, **21,** 343–346.

Montgomery, D. & Dietrich, W.E. (1988) Where do channels begin? *Nature*, **336,** 232–234.

Muhs, D.R. (1983) Quaternary sea-level events on northern San Clemente Island, California. *Quat. Res.*, **20,** 322–341.

Muhs, D.R. (1985) Amino acid age estimates of marine terraces and sea levels, San Nicolas Island, California. *Geology*, **13,** 58–61.

Muhs, D.R., Kennedy, G.L. & Rockwell, T.K. (1994) Uranium series ages of marine terrace corals from the Pacific coast of North America and implications for last-interglacial sea level history. *Quat. Res.*, **42,** 72–87.

Paola, C. & Borgman, L. (1991) Reconstructing random topography from preserved stratification. *Sedimentology*, **38,** 553–565.

Rockwell, T.K., Muhs, D.R., Kennedy, G.L., Hatch, M.E., Wilson, S.M. & Klinger, R.E. (1989) Uranium-series ages, faunal correlations and tectonic deformation of marine terraces within the Agua Blanca fault zone at Punta Banda, northern Baja California, Mexico. In: *Geologic Studies in Baja California* (Ed. by P.L. Abbott), pp. 1–16. Society of Economic Paleontologists and Mineralogists (Pacific Section), Book 63, Los Angeles.

Rosenbloom, N.A. & Anderson, R.S. (1994) Geomorphic decay of marine terraces, Santa Cruz, California. *J. Geophys. Res.*, **99,** 14013–14029.

Sadler, P.M. (1981) Sediment accumulation rates and the completeness of stratigraphic sections. *J. Geol.*, **89,** 569–584.

Seidl, M.A. & Dietrich, W.E. (1992) The problem of channel erosion into bedrock. *Catena, Suppl. 23, 101–124.*

Shackleton, N. & Opdyke, N. (1973) Oxygen isotope and paleomagnetic stratigraphy of equatorial Pacific core V28–238. Oxygen isotope temperatures on a 105 and 106 year time scale. *Quat. Res.*, **3,** 39–55.

Small, E.E., Anderson, R.S. & Finkel, R. (1997) Erosion rates of summit flats using cosmogenic radionuclides. *Earth Planet. Sci. Lett*, **150,** 413–425.

Sunamura, T. (1992) *Geomorphology of Rocky Coasts*. John Wiley & Sons, New York.

Talling, P.J., Stewart, M.D., Stark, C.P. & Gupta, S. (1997) Regular spacing of drainage outlets from linear fault blocks. *Basin Res.*, **9,** 275–302.

Turcotte, D.L. & Bernthal, M.J. (1984) Synthetic coral-reef terraces and variations of Quaternary sea level. *Earth Planet. Sci. Lett*, **70,** 121–128.

Valensise, G. & Ward, S.N. (1991) Long-term uplift of the Santa Cruz coastline in response to repeated earthquakes along the San Andreas fault. *Bull. Seismol. Soc. Am.*, **81,** 1694–1704.